

UNCLASSIFIED

Defense Technical Information Center
Compilation Part Notice

ADP010505

TITLE: Aero-Mechanical Design Methodology for
Subsonic Civil Transport High-Lift Systems

DISTRIBUTION: Approved for public release, distribution unlimited

This paper is part of the following report:

TITLE: Aerodynamic Design and Optimisation of
Flight Vehicles in a Concurrent
Multi-Disciplinary Environment [la Conception et
l'optimisation aerodynamiques des vehicules
aeriens dans un environnement pluridisciplinaire
et simultane]

To order the complete compilation report, use: ADA388284

The component part is provided here to allow users access to individually authored sections of proceedings, annals, symposia, ect. However, the component should be considered within the context of the overall compilation report and not as a stand-alone technical report.

The following component part numbers comprise the compilation report:

ADP010499 thru ADP010530

UNCLASSIFIED

Aero-Mechanical Design Methodology for Subsonic Civil Transport High-Lift Systems

C.P. van Dam, S.G. Shaw, J.C. Vander Kam, R.R. Brodeur
 Department of Mechanical and Aeronautical Engineering
 University of California
 One Shields Ave
 Davis, CA 95616-5294, USA

P.K.C. Rudolph
 PKCR, Inc.
 Seattle, WA 98166, USA

D. Kinney
 NASA Ames Research Center
 Moffett Field, CA 94035-1000, USA

Abstract:

In today's highly competitive and economically driven commercial aviation market, the trend is to make aircraft systems simpler and to shorten their design cycle which reduces recurring, non-recurring and operating costs. One such system is the high-lift system. A methodology has been developed which merges aerodynamic data with kinematic analysis of the trailing-edge flap mechanism with minimum mechanism definition required. This methodology provides quick and accurate aerodynamic performance prediction for a given flap deployment mechanism early on in the high-lift system preliminary design stage. Sample analysis results for four different deployment mechanisms are presented as well as descriptions of the aerodynamic and mechanism data required for evaluation. Extensions to interactive design capabilities are also discussed.

Introduction:

The aero-mechanical design of high-lift mechanisms is an important part of the total aircraft design process. In order to insure acceptable performance, a great deal of analysis must be done from both the aerodynamics and mechanism standpoints. Not only do high-lift systems account for 5-11% of the total aircraft cost for a typical subsonic transport, but high-lift configuration performance is important because it can have a large impact on the total mission performance of an aircraft. For example, an increase of 1% in take-off lift-to-drag ratio, L/D , for a typical long-range twin-engine subsonic transport can result in a payload increase of 2800 lb or a 150 nm increase in range (Meredith, 1993). Similarly, an increase of 1.5% in maximum lift coefficient, $C_{L,max}$, at a given approach speed can result in an additional 6600 lb of payload (Meredith,

1993). These analyses reveal the potential gain from detailed high-lift system design, but the actual details of how to obtain optimal aerodynamic performance with a given high-lift system can be tedious at best. A multidisciplinary approach has been developed in order to quickly and accurately predict the constrained performance characteristics of a trailing-edge flap system. This technique allows a general database of aerodynamic performance to be integrated directly into the mechanism design and analysis. This is accomplished through the use of a commercial software package along with a custom 'loads routine' which incorporates aerodynamic data from computational fluid dynamics (CFD) or experiment. Aerodynamic data is combined with kinematic data of the flap mechanism during deployment. The current method is limited to 2-D mechanisms, but can obviously be adapted to a 3-D wing. The aerodynamic database may be experimental or computational.

Aerodynamic Database:

The development of an aerodynamic database is the most time intensive portion of the process. The method of development of this database is up to the user, whether through CFD or experimental methods. The database should contain 2-D airfoil performance data as a function of flap gap and overlap. These flap geometry parameters are defined in Figure 1a. Note that flap gap is defined as the minimum distance between any point on the main element and the flap instead of the more common minimum distance from the trailing edge of the main element to the flap. The reason for adopting this slightly different definition is to allow better tracking of the distance between the two elements for flap settings with large overlaps.

Defining the aerodynamic database as a function of flap gap and overlap allows it to be used for any mechanism based on the location and orientation of the flap in relation to the main element of the airfoil. Clearly, this can be a large amount of data. For instance, in order to analyze five flap settings each ranging from 0 - 0.12c overlap and from 0 - 0.03c gap (where c is the chord of the cruise airfoil) at a resolution of 0.005c for each parameter, one arrives at 875 separate cases which must be analyzed. This number may be reduced through educated guesses at the probable gap and overlap ranges attainable at each flap setting. This data is all for a single angle of attack.

In this report, an angle of attack of 8° was selected in order to demonstrate the usefulness of the methodology. This angle is fairly representative for both take-off and approach/landing conditions. In the present study the aerodynamic data was compiled using INS2D which solves the incompressible Reynolds-averaged Navier-Stokes equations on structured, overset meshes (Rogers & Kwak, 1991). This flow solver has been extensively validated for multi-element flows and shown to provide sufficient accuracy in the prediction of these flows (Rogers, 1994). To resolve the complex flow phenomena related to high-lift aerodynamic components, a total of five meshes were used including a principal (background) mesh about the main element, a slat mesh, a flap mesh, and separate meshes for the main-element cove and the flap wake (Figure 1b). The high-lift configuration used is the Douglas LB-546 three element airfoil as shown in Figure 1. The airfoil in the cruise configuration has a maximum thickness-to-chord ratio of 11.55%. The slat chord is 14.48% and the flap chord is 30% of the cruise chord. This multi-element airfoil has been the subject of extensive experimental and computational studies by several researchers (Klausmeyer & Lin, 1997).

In order to further validate the ability of INS2D to predict the aerodynamic performance of this configuration as well as capture changes due to small flap rigging adjustments, a comparison with experimental results is performed. A study by Frank Lynch and his colleagues at the Boeing Company (Lynch, 1995) provides performance changes as a function of flap gap and overlap for this high-lift configuration. Comparisons in terms of ΔC_l and ΔC_d between the experimental results and the predictions based on INS2D are presented in Figure 2. The baseline configuration for this study is the airfoil with a flap gap of 1.27%c and overlap of 0.25%c (gap and overlap as defined by Lynch, 1995). From these comparisons, it is clear that though the values of ΔC_l and ΔC_d do not match up perfectly, the trends are generally very similar. Due to the

nature of the design methodology presented in this report, correct trends, specifically those in optimum flap gap and overlap, are sufficient for the technique to be useful. The disagreement between the experimental results and those predicted by INS2D in Figure 2 may be due to discrepancies in the transition location on the various elements of the high-lift system. No transition data is provided in the experimental results and the validation was done prior to integration of a transition prediction algorithm into INS2D. For the validation, transition was specified at the suction peaks of each element.

The geometries of the main-element cove and shroud as well as the flap of the LB-546 three element configuration were modified to allow retraction of the flap and to provide sufficient space for the flap actuation mechanism (Shaw, 1998). Comparison of the aerodynamic characteristics of the original and the modified configuration indicated only minor differences as a result of these geometry changes. Data is compiled in terms of the total 2-D airfoil lift coefficient, C_l , drag coefficient, C_d , and lift-to-drag ratio, $(L/D)_{2-D}$ as well as flap loading for flap settings of 5° , 10° , 20° , 30° , and 35° as functions of flap gap and overlap. The slat has three positions: stowed, take-off, and landing. The take-off position is used for the 5° - 20° flap settings and the landing position used for flap settings of 20° - 35° . Note that this results in two sets of data for the 20° flap setting. A Reynolds number based on the cruise airfoil chord and freestream conditions of 15.7 million was used based on typical approach speeds and wing chord lengths seen in current transport aircraft. In Figure 3 a very small portion of the database is shown for the configuration with 20° flaps and the slat in the landing position.

Figure 3a depicts the lift of the configuration at $\alpha=8^\circ$ and $Re=15.7$ million as a function of flap gap and overlap. Optimum lift performance appears to occur for overlap and gap settings of approximately 0.010c and 0.015c, respectively. However, the performance is rather sensitive to small variations in the gap setting at these small overlap settings. Figure 3b depicts the $(L/D)_{2-D}$ of the high-lift configuration as a function of flap gap and overlap. Interesting to note are the need for the overlap to be small (0-0.02c) to maximize $(L/D)_{2-D}$, and the significant effect of flap gap on $(L/D)_{2-D}$ especially at small overlaps.

Due to the sensitivity of take-off lift-to-drag ratio to drag prediction, some attention must be paid to transition location on the airfoil elements. In the development of the database used in this study, transition is specified on each element at the suction peak of the pressure distribution. Since the development of this database, a transition prediction algorithm has been included within the INS2D

flow solver that makes it possible to determine transition location automatically as the flow solution converges. This methodology identifies several factors that influence laminar boundary layer stability, and hence, lead to boundary layer transition. In two dimensional airfoil flows, where surfaces are generally smooth and freestream turbulence levels are low, transition is governed by Tollmien-Schlichting (TS) instability, laminar separation or turbulence contamination (Kusunose & Cao, 1994). The latter phenomenon is often overlooked, but can be important when, for instance, the flap boundary layer is contaminated by the wake of the main element and/or the slat (van Dam et al, 1997).

TS instabilities, or TS waves, can be analyzed with the e^N transition criterion. This criterion is based on the growth of the TS instabilities in the laminar boundary layer. These instabilities, which are initially damped so that disturbances are suppressed, become neutrally stable at some critical point. After this point the disturbances begin to amplify. When they amplify beyond a certain level, boundary layer transition is imminent. The log of this amplification level is commonly referred to as the 'N-factor' and usually taken as $N=9$. However, depending on ambient conditions, the N-factor can be as high as $N=13.5$ (Horstmann et al, 1990).

In INS2D, the N-factor is analyzed with an empirical e^N method which relates the N-factor to the local boundary layer properties, shape factor and momentum thickness (Drela & Giles, 1987). Boundary layer properties are obtained through direct integration of the velocity profiles, which requires a highly resolved boundary layer mesh, or through an integral boundary layer method, which requires only the pressure distribution.

In addition, local skin friction is calculated so that laminar separation can be detected. Once laminar separation is detected through a negative skin friction value it is assumed a small bubble will form. To account for the bubble length, an empirical bubble model is used to delay the onset of transition beyond the point of separation (Schmidt & Mueller, 1989). This feature is especially useful for flows with low Reynolds numbers where laminar bubbles can be significant to the flow development.

Transition by turbulence contamination is predicted naturally by using the Spalart-Allmaras turbulence model (Kusunose & Cao, 1994). In the Spalart-Allmaras model, a source term is added at the transition onset point. This source term is only non-zero in the turbulent boundary layer or turbulent wake. If a turbulent wake intersects a trailing laminar boundary layer, this source term may already be non-zero. Hence, transition may automatically be triggered upstream of the specified location.

Overall, promising results have been obtained from this type of study (Kusunose & Cao, 1994, Duque et al, 1999). The present transition prediction formulation has been applied to the NLR 7301 flapped airfoil. The test was conducted for the airfoil with a flap angle of 20° , flap gap of $0.026c$ and flap overlap of $0.053c$ at a chord Reynolds number of 2.51 million and an angle of attack of 6° . This particular airfoil configuration was chosen due to the extensive experimental data available, which includes transition measurements (van den Berg, 1979). The predicted transition locations are compared to the experimentally observed locations in Figure 4. On the lower surface of the main element, transition is calculated within the range observed in the experiment, whereas transition on the upper surface is predicted slightly aft of the observed range. Transition on the flap element is predicted slightly ahead of that seen in the experimental observations. In general, the calculated transition points agree well with experimental observations.

The predicted lift and drag coefficients are in good agreement with the experimental results. Experimental results found $C_l=2.42$ while INS2D with transition free found $C_l=2.44$. The experimental drag results show $C_d=0.0229$ while INS2D with transition free found $C_d=0.0217$. Especially the drag results, although not in perfect agreement, correspond much better with the experimental data than previous Navier-Stokes results obtained for the same configuration (van Dam, 1999).

Mechanism Simulation:

Mechanism simulation is accomplished through the Pro/Mechanica™ software package. This is a kinematics package capable of simulating the motion of user-defined mechanisms using time-based equations of motion. It may be used in conjunction with the Pro-Engineer™ CAD package or as a stand-alone tool. Many different types of linkages, joints, drivers, and connections are available to the user as well as the capability to incorporate custom loading programs written in FORTRAN or C. The mechanisms used to deploy trailing-edge flaps lend themselves very well to the use of this package for analysis of their action. Assembly of the mechanisms in Mechanica is a point-and-click process similar to traditional CAD techniques. Four sample mechanisms are depicted in Figure 5.

Figure 5a depicts a four-bar linkage designed to increase the amount of Fowler motion at lower flap setting angles. This results in the Aggressive Four-Bar Linkage (Rudolph, 1998). The basis for this mechanism is derived from the initial Boeing design for the 777 outboard trailing-edge flaps. Figure 5c depicts a Link-Track mechanism based

on the Airbus 320 design (Rudolph, 1998). Additionally, a Conservative Four-Bar Linkage (Figure 5b) with less initial Fowler motion than the Aggressive Four-Bar Linkage and a Moveable Track Link-Track (Figure 5d) were modeled from the report by Rudolph. All of these mechanisms show rotary actuators driving the forward link. The rotary drive assembly is classically mounted to the rear spar of the wing, beneath the shroud assembly. Alternative means of driving flap mechanisms are available, but the rotary drive is very common in present designs due to its low maintenance requirements. There are many additional factors that enter into the design of these mechanisms. Side-load handling, conical motion in the 3-D configuration, and fairing size and movement are just a few of the issues that must be addressed. Since the aerodynamic performance of the flaps is the only concern in this study, the mechanism links are modeled as perfectly rigid and massless while the joints are frictionless. This modeling of the mechanisms used for the motion simulation are highly simplified, but sufficient for accurate flap position analysis. Capabilities for more detailed structural analysis are available, but are not part of the present study.

Pro/Mechanica™ is capable of tracking locations, velocities, and orientations of points and bodies in terms of global or local reference frames, but in order to keep track of the gap and overlap measures used in the aerodynamic database, a custom subroutine is required. This consists of an in-house code which interacts with the Mechanica simulation at each time step. The code takes in from Mechanica the flap angle and location of the trailing-edge of the flap and then calculates the gap and overlap based on the known airfoil coordinates. Based on this information, the subroutine then looks up aerodynamic performance based on the flap gap, overlap, and angle. An interpolation routine is included in this procedure. This information is then returned to Mechanica and is able to be presented by the on-board Mechanica plotting package. One may then analyze airfoil C_l , C_d , and $(L/D)_{2-D}$ as well as other parameters such as pitching moment coefficient, C_m , driver torque coefficient, C_T , and forces in the various mechanism linkages as a function of flap angle. Simulation time varies with the desired amount of time resolution and the speed of one's processor, but rarely exceeds a minute per mechanism for the full flap deflection range on older desk-top systems.

Analysis Results:

Results of the mechanism analysis are easily viewed directly from Mechanica. Figure 6 presents performance results for the four aforementioned mechanisms compared with the highest possible performance obtainable

at each flap angle.

Figure 6a presents C_l performance for the four mechanisms. The discontinuity in the data at 20° is due to the fact that this flap setting was analyzed with the slat in both the landing and take-off positions. Note also that since the mechanism simulation is based on discrete time steps, data points do not necessarily fall exactly on deployment angles for which aerodynamic performance data exists. One must specify an envelope around the desired flap angle within which the simulation will output data for that angle. This accounts for the off-set seen in some of the mechanism performance data points. Further refinement of the time step and data point envelopes reduces this off-set, but significantly increases simulation time. The current time resolution provides data outputs within less than one degree of the desired flap deployment angles.

The differences in lift characteristics between the mechanisms are modest, with the largest variation in C_l being approximately 0.15. This is still an appreciable amount considering the previous examples on the impact small changes can have on typical airliners today. A more interesting result is presented in Figure 6b. This plot presents the $(L/D)_{2-D}$ performance of the four mechanisms compared to the maximum attainable performance. Lift-to-drag ratio is an important performance parameter for airplanes at take-off where the aerodynamic design is aimed at finding an acceptable compromise between lift capability at take-off and stall angles of attack and L/D efficiency (Flaig & Hilbig, 1993). For airplanes on approach for landing, L/D is less important. It may even be possible that the L/D of single-slotted flap high-lift devices may be too good at flap settings used during landing (Flaig & Hilbig, 1993). Obviously, the performance of a 2-D high-lift configuration differs from that in 3-D, but beginning with a good idea of which mechanisms perform well in 2-D will shorten the 3-D design and analysis process.

From Figure 6b, it is clear that no mechanism is able to achieve optimum $(L/D)_{2-D}$ for all flap settings, especially not at the lower flap angles of 5° to 20° where lift-to-drag ratio is important for good take-off performance. The best performers between 10° and 20° are the two link-track mechanisms with a $\Delta(L/D)_{2-D}$ of about 8 below optimum at each flap setting. At 5°, the Moveable Track Link-Track is the best performer with a $\Delta(L/D)_{2-D}$ of about 5 below optimum. It is important to note that the two mechanisms with the best Fowler motion progression show a $\Delta(L/D)_{2-D}$ of about 10 higher than the poorest of the four mechanisms considered at the lower flap settings. The take-off lift-to-drag ratio of a simple hinge would be considerably worse.

A third parameter of interest is the actuator torque required to deploy the flap mechanisms. Figure 7 presents actuator torque coefficient as a function of flap setting. Actuator torque is important for sizing the actuator and mechanism as well as determining the behavior of the flap mechanism. It is important to avoid load reversal throughout the deployment range of the flaps. Load reversal is said to occur when the loading on the actuator changes from a stowing load to a deploying load or vice versa. Load reversal can lead to flutter and fatigue problems. Additionally, in the case of structural or mechanical failure, trailing-edge flaps must stow themselves. The sign of actuator torque is indicative of whether or not this will happen. From Figure 7, one sees that the Aggressive Four-Bar Linkage mechanism comes close to actuator torque reversal at the 35° flap setting.

Analysis Benefits:

Final product price is often determined within the preliminary design phase through specification of configuration, mission, and size. The ability to accurately predict performance of a candidate configuration early on shortens development time and ensures a quality design.

Note that any known flap mechanism can move a flap from its stowed position to a desired landing position. Therefore, the flap mechanism has very little influence on landing performance. However the various flap mechanisms will cause significant differences in Fowler motion for typical take-off flap settings, thus greatly impacting take-off L/D . Mechanism choice also impacts complexity, actuation power requirements and weight which affect cost and overall airplane weight. Different flap mechanisms require different flap support fairing sizes which impact cruise and low speed drag as well as weight.

The results presented in the preceding figures may be obtained without knowledge of the flap deployment mechanism details. Early on, a designer may look at several candidate mechanism configurations and narrow the field of viable mechanisms through this type of analysis. For example, if airplane climb-out performance is of concern, from Figure 6b one may be able to eliminate several mechanisms right away based on their $(L/D)_{2-D}$ performance at low flap settings. This kind of information early on in the design process can aid the designer in selecting a mechanism type sooner rather than later. These simple mechanism models also give the designer an idea of the complexity and size of the final mechanism. An important issue to cruise performance is the flap mechanism fairing. The fairing size for each mechanism may be determined in a relative sense through these simple models by examining

the configuration's vertical dimensions.

Design and Optimization:

In addition to providing analysis, this methodology is also capable of automated mechanism design. Using the on-board Mechanica design study features, mechanisms may be modified in order to improve performance. This requires some additional coding in the custom loads routine and the specification of design parameters within Mechanica. Successful optimizations have been conducted using airfoil C_l and for $(L/D)_{2-D}$ as the objective function and the mechanism linkage lengths as the design parameters. In this way, a designer is able to take a general mechanism type and tailor it to provide improved aerodynamic performance based on the mission goals. For example, one may define the objective function as $(L/D)_{2-D}$ at 5° and 10°, and C_l at the higher flap settings. These parameters can be combined into a single design factor by taking the root mean square (RMS) or some other average of the desired parameter over the range of flap settings. Then the mechanism linkages are changed in order to maximize that parameter.

An example of this type of optimization is seen in Figure 8. The aforementioned Aggressive Four-Bar Linkage is modified, or down-graded, to provide less C_l performance by altering the lengths of the driver arm and the aft-most link. The resulting performance is seen in Figure 8. This initial modification provides a less than optimal starting mechanism for the optimizer to adjust. The optimization routine was then set to maximize the RMS of C_l at each of the flap settings (5°, 10°, 20°, 30°, 35°) by varying the lengths of the two previously mentioned mechanism links. Design constraints are that the stowed position remains unchanged, that the final flap angle must be within 0.5° of 35° and that the gap must remain positive. The latter constraint ensures that no interference between the flap and the main element will occur. From Figure 8, it is clear that improvements have been obtained in the lift performance especially at higher flap settings. At the 35° flap setting, C_l has been raised from 3.25 to 3.35 and from 2.95 to 3.15 at the 30° setting. The focus on the higher flap settings is due in part to the relatively low sensitivity of C_l on gap and overlap at the lower settings as well as the fact that the displaced mechanism is still performing close to optimum at the lower settings. The nature of the objective function also allows for uneven improvements. Since the objective function is defined as the RMS of C_l at each flap deployment angle, optimization may not be focused evenly throughout the deployment range. In order to counter-act this phenomenon, weighting factors may be added to the individual C_l 's, thus shifting the focus of the optimization

routine.

Though thorough validation of the optimization process remains to be completed, the technique shows great promise especially in the preliminary design of these types of flap deployment mechanisms. One may use this method to determine whether or not a certain mechanism layout has the potential to perform up to the desired standards before a final mechanism type is chosen.

Conclusions:

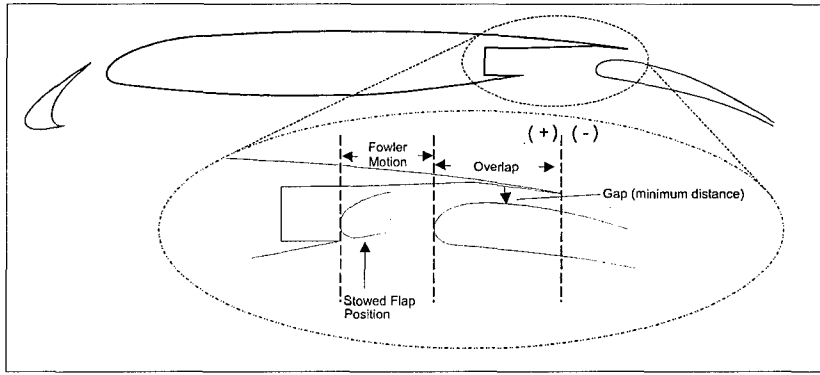
A multi-disciplinary design process such as the one presented here has great potential to decrease the amount of time and money spent in the preliminary design of trailing-edge flap mechanisms. The most time consuming segment of the study was the generation of an extensive aerodynamic database using CFD. The performance data contained in this database underscores the important effect of flap overlap/Fowler motion on $(L/D)_{2-D}$ efficiency especially for takeoff flap settings. Flap gap is also shown to have an important effect on $(L/D)_{2-D}$ especially at small overlaps. Once the aerodynamic database is developed, the designer may close in on a mechanism choice very quickly. Automated optimizations are possible and are being investigated further. This methodology is purely two-dimensional and the transition to 3-D mechanism design may alter performance evaluations and design constraints.

Acknowledgements:

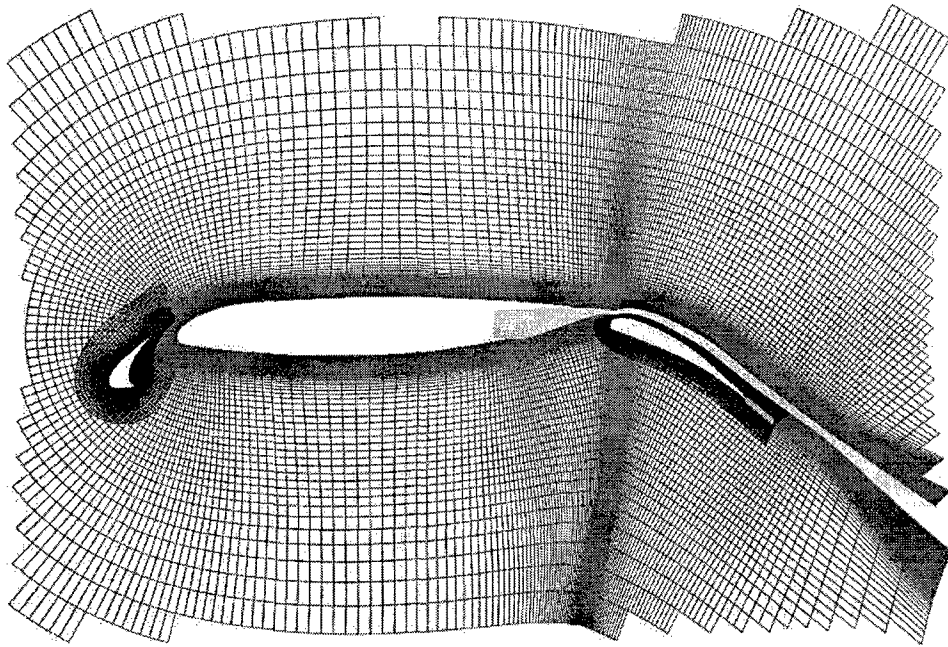
The efforts by van Dam, Shaw, and Vander Kam were supported by the NASA Ames Research Center (ARC) under Consortium Agreements NCC2-5188 and NCC2-5255. Brodeur was supported by the Sandia National Laboratories under Contract A0273. Rudolph was supported by ARC under Contracts A46374D(LAS) and A49736D(SLS).

References:

- Drela, M. and Giles, M.B., (1987) "Viscous-Inviscid Analysis of Transonic and Low Reynolds Number Airfoils," AIAA Journal, Vol. 25, No. 10, pp.1347-1355.
- Duque, E.P.N., van Dam, C.P., Brodeur, R.R., and Chao, D.D., (1999) "Navier-Stokes Analysis of Time-Dependent Flows about Wind Turbines," FEDSM99-S295-2, 3rd ASME/JSME Joint Fluids Engineering Conference, San Francisco, CA.
- Flaig, A. & Hilbig, R., (1993) "High-Lift Design for Large Civil Aircraft," AGARD CP 315, pp. 31-1 thru 31-12.
- Horstmann, K.H., Quast, A., and Redeker, G., (1990) "Flight and Wind-Tunnel Investigations on Boundary-Layer Transition," Journal of Aircraft, Vol. 27, No. 2, pp. 146-150.
- Klausmeyer, S.M. and Lin, J.C., (1997) "Comparative Results from a CFD Challenge over a 2D Three-Element High-Lift Airfoil," NASA TM 112858.
- Kusunose, K. and Cao, H.V., (1994) "Prediction of Transition Location for a 2-D Navier-Stokes Solver for Multi-Element Airfoil Configurations," AIAA Paper 94-2376.
- Lynch, F.T., (1995) "Subsonic Transport High-Lift Technology Review of Experimental Studies," AIAA Overview of High Lift Aerodynamics.
- Meredith, P.T., (1993) "Viscous Phenomena Affecting High-Lift Systems and Suggestions for Future CFD Development," AGARD CP 315, pp. 19-1 thru 19-8.
- Rogers, S.E., (1994) "Progress in High-Lift Aerodynamic Calculations," Journal of Aircraft, Vol. 31, No. 6, pp. 1244-1251.
- Rudolph, P.K.C., (1998) "Mechanical Design of High Lift Systems for High Aspect Ratio Swept Wings," NASA CR 1998-196709.
- Schmidt, G.S., and Mueller, T.J., (1989) "Analysis of Low Reynolds Number Separation Bubbles Using Semiempirical Methods," AIAA Journal, Vol. 27, No. 8, pp. 993-1001.
- Rogers, S.E. and Kwak, D., (1991) "An Upwind Differencing Scheme for the Steady-State Incompressible Navier-Stokes Equations," Applied Numerical Mathematics, Vol. 8, No. 1, pp. 43-64.
- Shaw, S.G., (1998) "An Improved Preliminary Design Methodology for High-Lift Systems for Subsonic Transport Aircraft," Master's Thesis, University of California, Davis.
- Spalart, P.R., and Allmaras, S.R., (1994) "A One-Equation Turbulence Model for Aerodynamic Flows," La Recherche Aéropatiale, No. 1, pp. 5-21.
- van Dam, C.P., Los, S.M., Miley, S., Roback, V.E., Yip, L.P., Bertelrud, A., and Vijgen, P.M.H.W., (1997) "In-Flight Boundary-Layer Measurements on a High-Lift System: Main Element and Flap," Journal of Aircraft, Vol 34, No. 6, pp. 757-763.
- van Dam, C.P., (1999) "Recent Experience with Different Methods of Drag Prediction," Progress in Aerospace Sciences, in print.
- van den Berg, (1979) "Boundary-layer Measurements on a Two-Dimensional Wing with Flap," NLR TR 79009U.



(a) Flap nomenclature



(b) Chimera grid

Figure 1: Douglas LB-546 three-element airfoil definition, flap nomenclature and computational grid definitions.

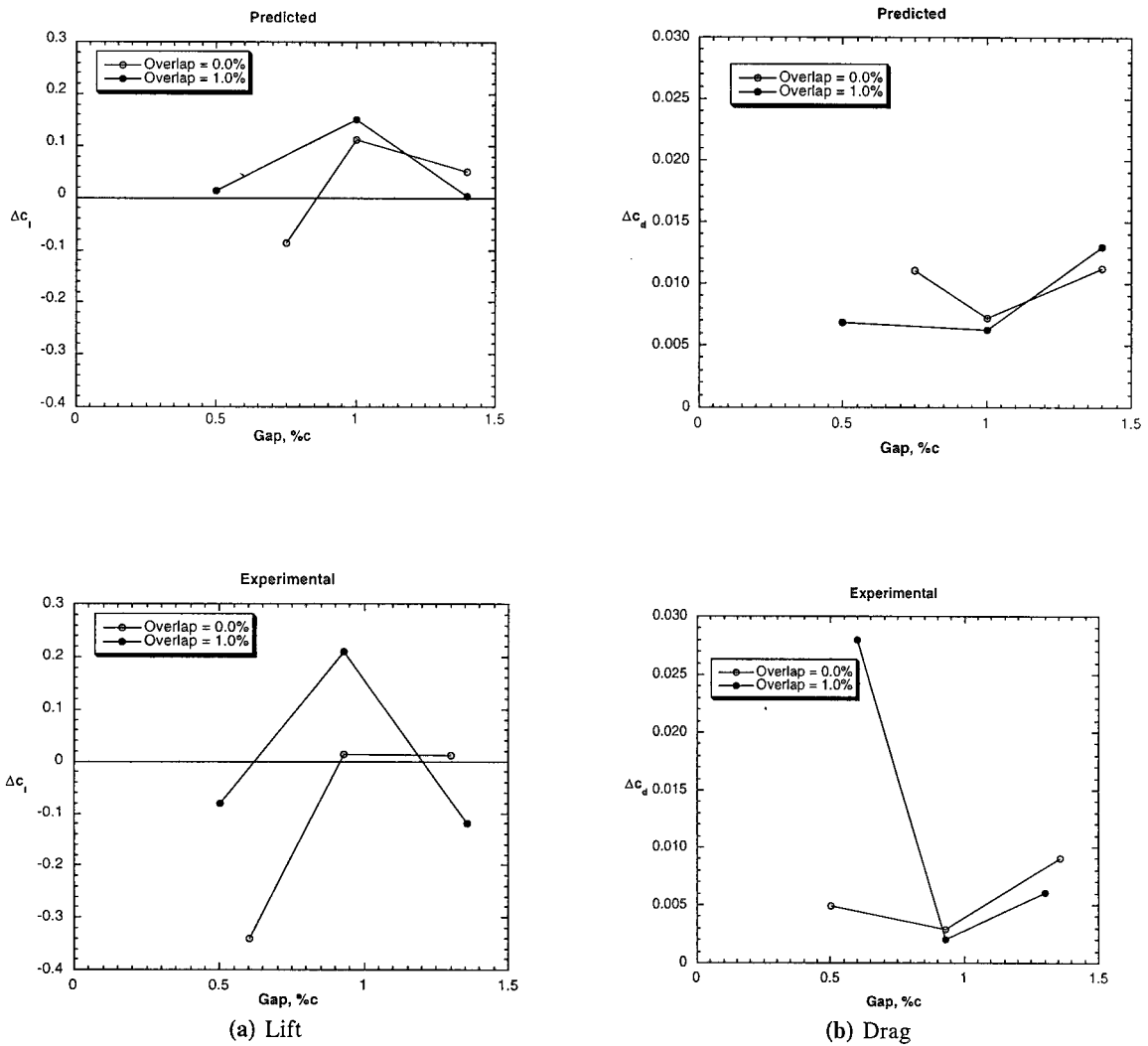
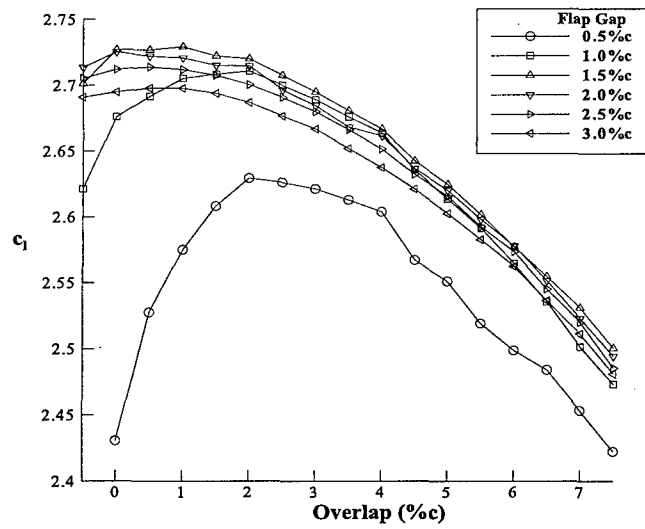
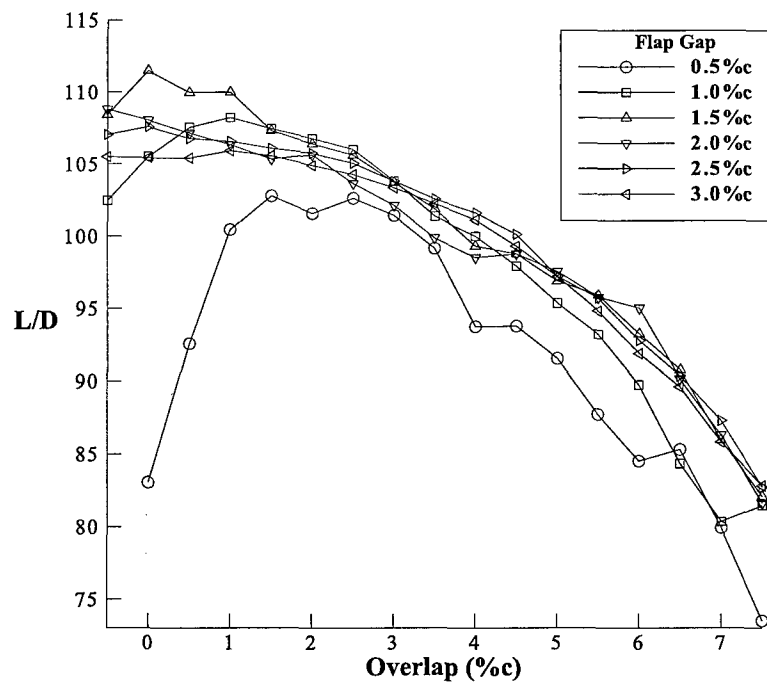


Figure 2: Comparison of predicted and measured effects of flap gap and overlap on lift and drag of LB-546 three-element airfoil at $\alpha=8^\circ$, $Re=9.0$ million, $\delta_f=35^\circ$. Baseline settings are flap gap of 1.27%c and overlap of 0.25%c.



(a) Lift



(b) Lift-to-drag ratio

Figure 3: Effect of flap gap and overlap for three-element airfoil at $\alpha=8^\circ$, $Re=15.7$ million, $\delta_f=20^\circ$, and slat in landing position.

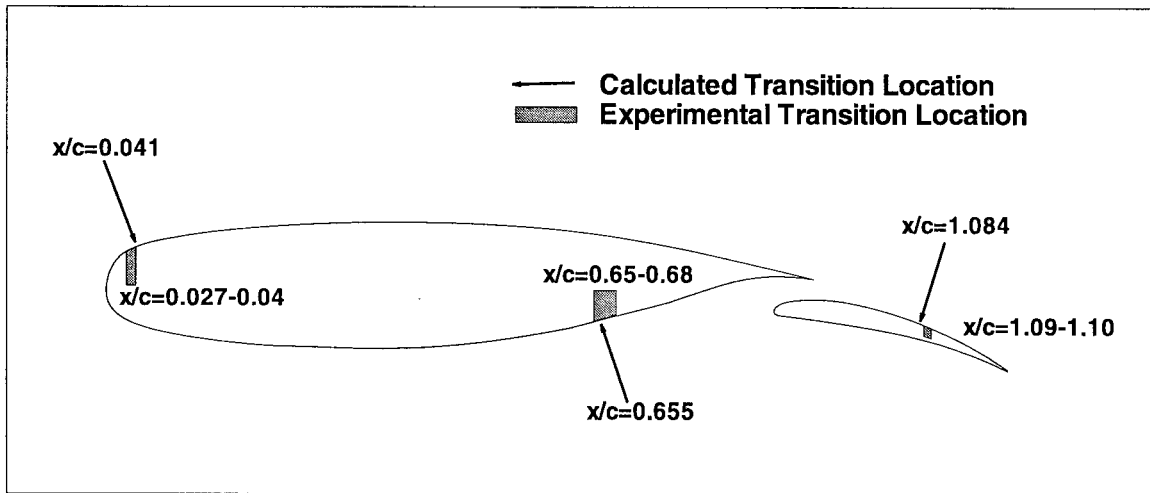


Figure 4: Comparison of predicted and measured transition locations for NLR-7301 flapped airfoil ($\delta_f=20^\circ$, flap gap=0.026c, flap overlap=0.053c) at $\alpha=6^\circ$ and $Re=2.51$ million.

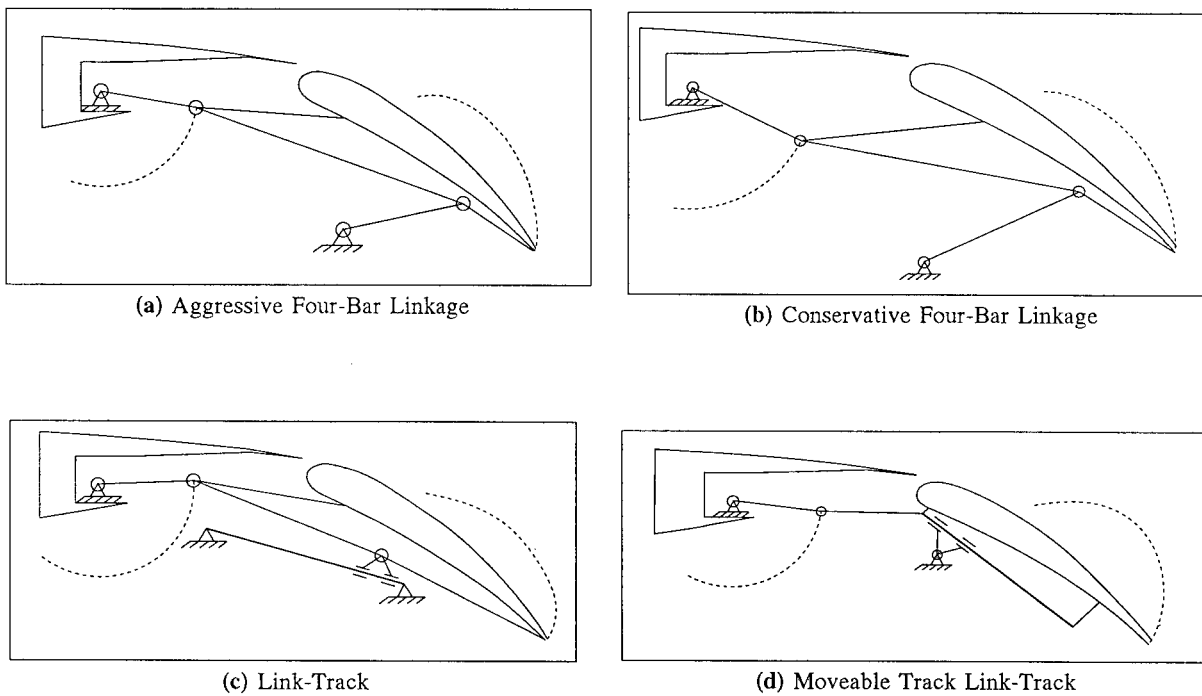
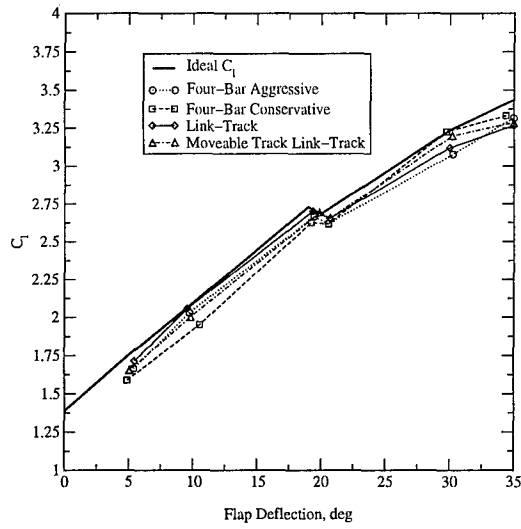
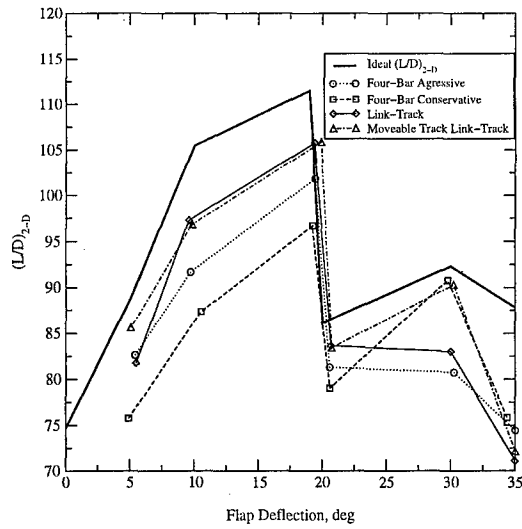


Figure 5: Flap mechanisms depicted at fully deployed setting ($\delta_f=35^\circ$).



(a) Lift



(b) Lift-to-drag ratio

Figure 6: Effect of mechanism on aerodynamic characteristics of three-element airfoil at $\alpha=8^\circ$, and $Re=15.7$ million.

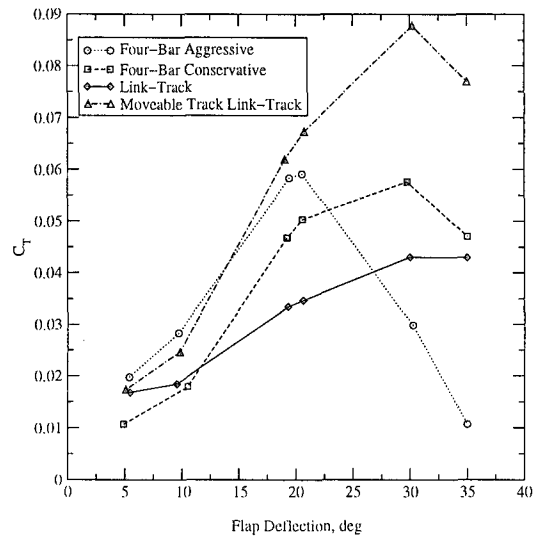


Figure 7: Effect of mechanism on actuator torque.

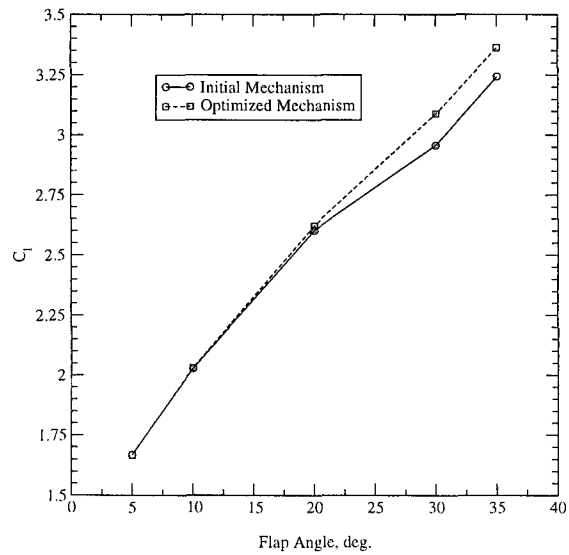


Figure 8: Lift optimization for the Aggressive Four-Bar Linkage, $\alpha=8^\circ$, $Re=15.7$ million.